

# The Impact of Temperature on the Electromagnet and Structural Optimization of a Solenoid Valve

Zhixiong Tang, Zhijun Feng\*

School of Mechanical and Automotive Engineering, Guangxi University of Science and Technology, Liuzhou 450200, Guangxi Zhuang Autonomous Region, China

\*Corresponding author: Zhijun Feng, fzjwywmz@163.com

**Copyright:** © 2024 Author(s). This is an open-access article distributed under the terms of the Creative Commons Attribution License (CC BY 4.0), permitting distribution and reproduction in any medium, provided the original work is cited.

**Abstract:** The mathematical model of the solenoid valve under varying temperatures is constructed to investigate its performance and enhance heat dissipation balance. The relationship between temperature and electromagnetic force is determined. Electrothermal coupling simulation using COMSOL is conducted, optimizing the outer diameter and length structure parameters of the coil. It is established that the heat dissipation of the coil is influenced by its outer diameter. Subsequently, based on optimized coil structure parameters, an orthogonal experimental design method combined with Ansys Maxwell is employed for simulation solution analysis to study the impact of structural parameters such as length, position, front and rear angles of the magnetic barrier ring in the iron core, armature length, and through-hole size on electromagnetic force. Optimal structural parameters are identified. Results indicate a decrease in steady-state electromagnet temperature by 3–4°C, an increase in the initial electromagnetic force by 32.63%, and a rise in the maximum electromagnetic force by 27.10%.

**Keywords:** Solenoid valve; Electromagnet; Temperature; Electromagnetic force

**Online publication:** January 18, 2024

## 1. Introduction

The solenoid valve, a crucial control element in hydraulic and pneumatic systems, has widespread applications in China's aerospace and navigation sectors. Despite the increasing maturity of solenoid valve design and application in recent years, practical issues such as reduced valve opening capacity at high temperatures or even design defects have been observed<sup>[1]</sup>.

The performance of the electromagnet, serving as the power source for the solenoid valve, plays a decisive role in determining its dynamic characteristics. However, it is worth noting that the coil itself generates heat during operation. As the temperature of the solenoid valve rises, so does its coil resistance, leading to a decrease in current flow. Moreover, thermal stress and expansion within the coil can affect the structure of the solenoid valve. Additionally, environmental factors may lead to wear or even melting of insulating paint on winding coils, ultimately resulting in failure<sup>[2-4]</sup>.

Researchers such as Liu and colleagues as well as Sun and colleagues<sup>[5,6]</sup>, among others, have constructed

physical field coupling models for solenoids and conducted finite element simulation analyses to investigate thermal characteristics under various working conditions, thereby identifying several factors influencing electromagnetic valve temperature distribution. Ren *et al.* studied temperature field distribution through multi-physical field simulation analysis combined with system dynamics hybrid modeling techniques. Their findings revealed significant impacts on dynamic characteristics due to changes caused by temperature fields affecting electromagnet structural parameters [7].

This study focuses on investigating temperature distribution and rise characteristics specific to a company's solenoid valves while proposing reasonable optimization strategies for structural parameters related to both coil and iron core.

## 2. Mathematical model of solenoid valve

The structure of a single-head electromagnetic directional valve primarily consists of a valve body, valve core, and electromagnet. Its operational principle involves energizing the coil, which generates electromagnetic force to propel the armature of the iron core. Overcoming spring force, frictional resistance, and hydraulic power, the spool moves to open the valve port. Consequently, oil enters through the inlet of the valve port into the flow channel within the valve body and exits from its outlet. Upon de-energizing the coil, electromagnetic force dissipates, and under spring action, the spool resets.

### 2.1. Equation of mechanical motion

$$\frac{md^2x}{dt^2} = F_m + F_k + F_p + F_f + F_v \quad (1)$$

Where:  $m$  is the quality of the spool;  $x$  is spool displacement;  $t$  is time;  $F_m$  is the electromagnetic force;  $F_k$  is the spring force;  $F_p$  is hydraulic power;  $F_f$  is the friction force on the valve core;  $F_v$  is the damping force on the spool.

Based on Maxwell's equations of electromagnetic field, the empirical formula of suction  $F_m$  when the leakage flux is ignored is as follows:

$$F_m = \frac{\phi^2}{2\mu_\delta S_\delta} = \frac{B^2 S_\delta}{2\mu_\delta} = \frac{(H\mu_\delta)^2 S_\delta}{2\mu_\delta} = \frac{(IN)^2 S_\delta \mu_\delta}{2\delta^2} = \frac{(\phi R_m)^2 S_\delta \mu_\delta}{2\delta^2} \quad (2)$$

Where:  $\phi$  is the coil magnetic flux;  $\mu_\delta$  is the permeability of the working air gap;  $B$  is the magnetic induction intensity at the working air gap;  $S_\delta$  is the cross-sectional area of the working air gap;  $H$  is the magnetic field strength at the working air gap;  $N$  is the number of coil turns;  $I$  is the coil working current;  $\delta$  is the length of working air gap;  $R_m$  is magnetoresistance.

### 2.2. Temperature

From Kirchhoff's voltage law, the current can be derived from the following equation:

$$U = i^2 R + \frac{d(Li)}{dt} \quad (3)$$

Where:  $U$  is the input voltage;  $i$  is the input current;  $R$  is coil resistance;  $L$  is the inductance of the coil.

### 2.3. Electric field

When the solenoid valve operates with a constant current, the coil generates Joule heat, the formula is as follows:

$$Q_V = \frac{i^2 R_0}{V} \quad (4)$$

Where:  $Q_V$  is the volume heat of coil resistance;  $R_0$  is coil resistance at  $T_0$  temperature;  $i$  is the current;  $V$  is the coil volume.

Coil resistance is related to conductivity and temperature, and the relationship is as follows:

$$R' = R_0 \left[ 1 + \frac{(T' - T_0) \gamma_c}{1 + T_0 \gamma_c} \right] \quad (5)$$

Where:  $R'$  is the coil resistance at  $T'$  temperature;  $\gamma_c$  is the temperature coefficient of resistivity.

In the case of constant operating voltage, the relationship between the electromagnetic force and temperature is as follows:

$$F_m = \frac{(IN)^2 \mu_0 S_\delta}{2\delta} = \frac{(UN)^2 \mu_0 S_\delta}{2\delta (R')^2} = \frac{U^2 N^2 \mu_0 S_\delta (1 + T_0 \gamma_c)^2}{2\delta R_0^2 [1 + T_0 \gamma_c + (T' - T_0) \gamma_c]^2} \quad (6)$$

The electromagnetic force, as indicated by **Formula (6)**, is influenced by various factors such as temperature, voltage, resistance, and working air gap. However, the neglect of magnetic leakage in **Formula (6)** leads to inaccurate calculation of the electromagnetic force. Therefore, it becomes imperative to employ the finite element method for comprehending the variations and distribution of electromagnet temperature and assessing the impact of electromagnet structural parameters on the electromagnetic force. Subsequently, optimization can be pursued to enhance solenoid valve performance.

### 3. Electromagnet temperature simulation

The focus of this paper is primarily on the heating situation of the electromagnet, thus temporarily excluding consideration of the influence of the valve body on heat dissipation. Additionally, this study is based on a specific Vickers solenoid valve as the research subject. A simplified two-dimensional model (as depicted in **Figure 1**) was established in COMAOL to simulate electric-magnetic-temperature field coupling, enabling an understanding of temperature variation and distribution within the electromagnet for conducting reasonable optimization.

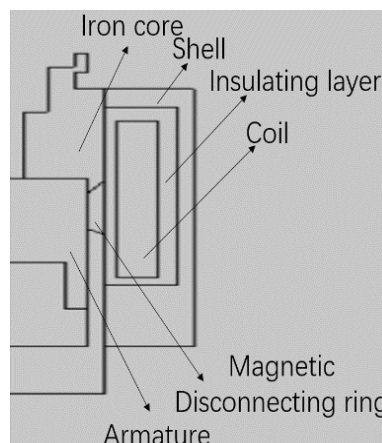


**Figure 1.** Electromagnet simplified model

According to **Figure 2**, it is evident that the coil winding and both ends of the iron core can reach temperatures as high as approximately 130°C and 100°C, respectively. From **Figure 3**, it can be observed that there is an approximate deviation of about 2°C between simulation and experimental results, while the temperature change curve remains essentially consistent. These findings validate the severity of coil heating and emphasize the necessity to avoid using PWM for voltage adjustment in solenoid valves, ensuring stable current output. Failure of solenoid valves may occur due to power domain reduction under extreme circumstances. Therefore, a comprehensive investigation into factors influencing solenoid temperature becomes imperative.

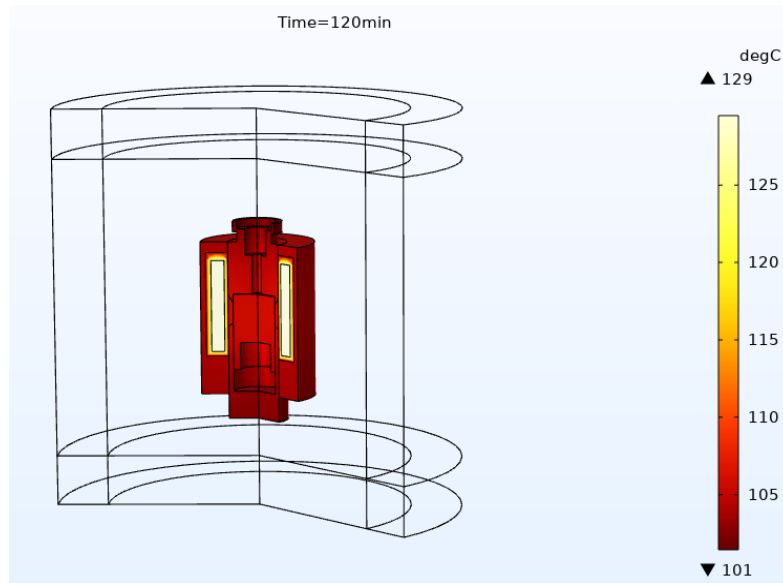


**Figure 2.** Steady-state temperature distribution of electromagnet

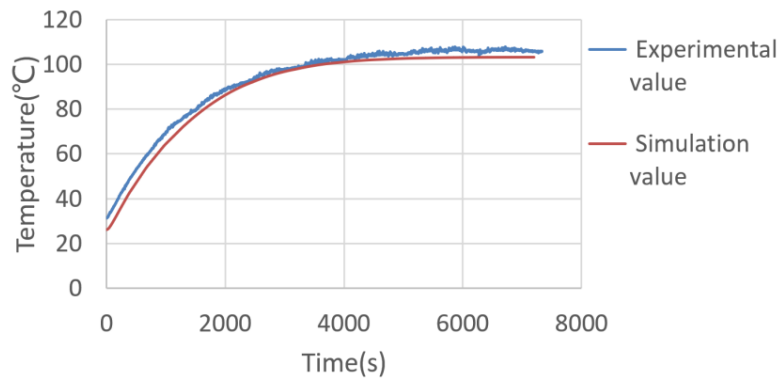


**Figure 3.** Comparison of experimental and simulated surface temperature of shell side

Numerous factors impact the temperature of the electromagnet, including input voltage, coil resistance, and ambient temperature. This paper focuses on studying and analyzing the structural parameters of the coil as influential factors on temperature while temporarily keeping the size of the iron core unchanged. Consequently, particular attention is given to examining how variations in the outer radius and height of the coil affect its temperature.

The analysis of **Figure 4** indicates that the impact of shell height on electromagnet heat dissipation is not significant. However, an appropriate increase in shell radius can effectively reduce the temperature rise rate and steady-state temperature. Considering the close proximity (2 mm) between the solenoid valve’s oil port surface

and coil, a 1.5 mm increment in shell radius is necessary to prevent interference with the installation valve block during operation.

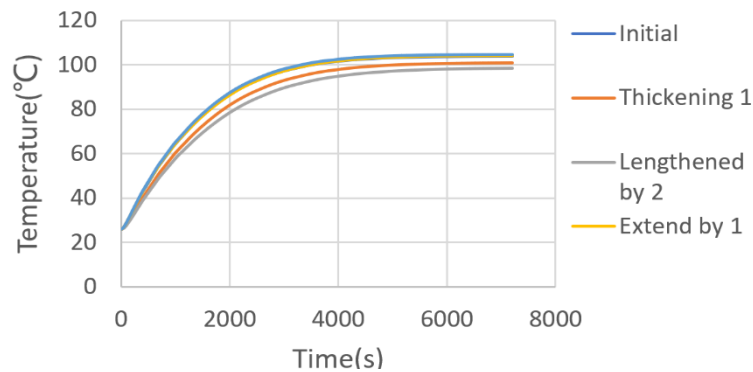


**Figure 4.** Changes in shell radius and height

#### 4. Electromagnetic force simulation optimization

According to the simulation results and **Formula (6)** mentioned above, increasing the shell radius can effectively reduce the steady-state temperature of the electromagnet while simultaneously enhancing the electromagnetic force when heat dissipation is balanced. To further augment the initial thrust in heat dissipation balance (which corresponds to the furthest effective stroke of the armature), this paper proposes modifying the structural parameters of the iron core. Additionally, based on Ansys Maxwell simulation, **Figure 1** illustrates a simplified model of the electromagnet. The current applied is 0.75A (representing its steady-state value when a solenoid valve is supplied with a voltage of 24 V for simulating operation until heat dissipation reaches equilibrium).

The experimental and simulated magnetic curves in **Figure 5** exhibit a similar trend, albeit with some discrepancies. These errors may arise from the disparity between the simplified model of the electromagnet and its real counterpart, as well as deviations in the relevant parameters of the magnetic material employed in the simulation compared to those of the actual object.

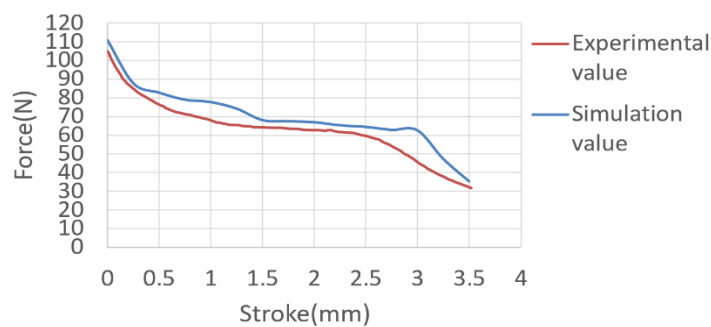


**Figure 5.** The experimental 0.75 A electromagnetic force curve is compared with the simulated curve

##### 4.1. Electromagnet core optimization

The electromagnetic force is influenced by various factors, including the number of coil turns and the working air gap. Additionally, the magnetic insulation ring, magnetic insulation angle, and structural parameters of the armature also impact the electromagnetic force. Therefore, it is necessary to employ the finite element method for calculation and analysis. The armature serves as a crucial moving component within the iron core, while

the separator ring plays a key role in dividing the magnetic circuit in electromagnets. Consequently, optimizing the structural parameters of both the armature and separator ring primarily constitutes the focus of this paper. The structure diagram of the armature and static core is presented in **Figure 6**, with a selection of 13 factors. These factors include the variation in upper-end length ( $h_1$ ) denoted as ‘a,’ the variation in lower-end length ( $h_2$ ) denoted as ‘b,’ the change in bottom hole depth denoted as ‘c,’ the alteration in diameter of  $d_2$  represented by ‘d,’ the modification in diameter of  $d_1$  indicated by ‘e,’ the adjustment in the number of through-holes referred to as ‘f,’ and  $L_1$  (the distance from the center of  $d_2$  to the center of  $d_1$ ) changes designated as ‘g.’ Additionally, variations such as magnetic separation angles  $\alpha$  (‘h’) and  $\beta$  (‘i’), position changes for magnetic barrier ring (‘j’), thickness alterations for magnetic barrier ring (‘k’), parallel movement changes when face 2 remains stationary (‘l’), and parallel movement changes when face 1 remains stationary (‘m’) were included.

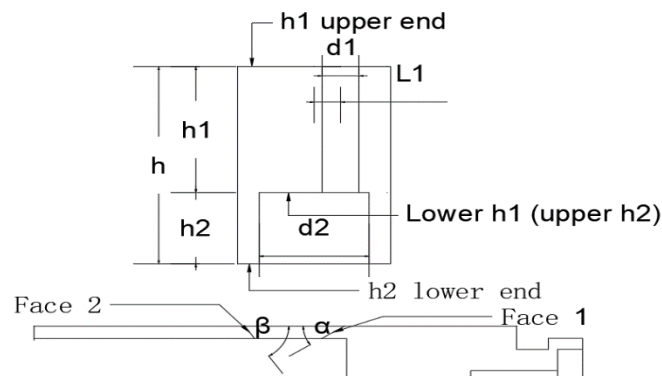


**Figure 6.** Armature and static core structure

In summary, a total of 13 factors were selected as variables for the optimization of electromagnetic force. Through single-factor analysis, four key factors that significantly affect the magnetic force were identified, namely the position of the magnetic barrier ring, the angle  $\alpha$  of the magnetic barrier, and the diameters  $d_1$  and  $d_2$  of the armature through the armature hole and bottom hole respectively. This study aims to identify a more suitable combination of structural parameters using orthogonal experimental design. Additionally, to enhance oil discharge from the electromagnet armature cavity, only diameter  $d_1$  remains unchanged while three levels are chosen for each of the other three factors. Consequently, **Table 1** presents nine combinations arranged accordingly which are then used to calculate the model’s electromagnetic force through simulation. Different simulation results have been obtained based on different combinations as shown in **Table 2**.

**Table 1.** Orthogonal experiment table  $L_9 (3^3)$

Number	e (mm)	h (mm)	j
1	12	Left shift 0.3	$36^\circ$
2	12	Left shift 0.4	$34^\circ$
3	12	Left shift 0.5	$35^\circ$
4	11	Left shift 0.3	$34^\circ$
5	11	Left shift 0.4	$35^\circ$
6	11	Left shift 0.5	$36^\circ$
7	10	Left shift 0.3	$35^\circ$
8	10	Left shift 0.4	$36^\circ$
9	10	Left shift 0.5	$34^\circ$

**Table 2.** The initial magnetic force value under different combinations

Number	1	2	3
Initial magnetic force (N)	37.473	54.453	54.774
Number	4	5	6
Initial magnetic force (N)	46.249	48.910	49.398
Number	7	8	9
Initial magnetic force (N)	42.507	43.868	60.707

The simulated initial thrust of the original structure is 35.205 N, as depicted in **Figure 5**, indicating that all combinations listed in **Table 2** meet the requirements. However, altering the structural parameters not only affects the initial thrust but also influences the suction force at other positions accordingly. Hence, it is essential to consider whether the electromagnetic force at these points satisfies the requirements for achieving the desired results, as illustrated in **Figure 7**. From **Figure 7**, it can be observed that some position points exhibit a decrease of approximately 2 N in optimized magnetic force compared to the original magnetic force, despite the impact being negligible. Among them, number 1 experiences a minimal increase in initial magnetic force while number 8 surpasses number 7 in terms of initial magnetic force magnitude. Consequently, selecting number 8 leads to a boost of approximately 24.607% in its initial magnetic force without significantly affecting the maximum electromagnetic force.

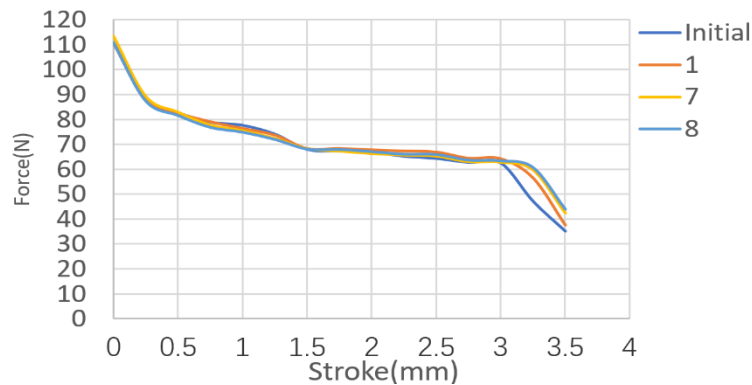


**Figure 7.** The optimized magnetic curve

## 5. Conclusion

The temperature field model is established, enabling a comprehensive understanding of the temperature distribution and temperature rise characteristics of the electromagnet. The variation in coil height has a negligible impact on heat dissipation, while an appropriate increase in coil outer diameter can effectively reduce the rate of temperature rise and steady-state temperature. By increasing the coil shell radius by 1.5 mm, its temperature can be reduced by 3–4°C. Through single-factor analysis of the structural parameters of the armature and magnetic barrier ring, four key factors influencing magnetic force are identified: the position of the magnetic barrier ring, magnetic barrier angle  $\alpha$ , armature hole diameter  $d_1$ , and bottom hole diameter  $d_2$ . Finally, utilizing an orthogonal design table helps identify a set of optimal structural parameters that result in a 24.607% increase in initial magnetic force with minimal change to the maximum electromagnetic force.

## Disclosure statement

The authors declare no conflict of interest.

## References

- [1] Shi Y, Pan Y, 2022, Calculation and Analysis of Influence of Temperature on Solenoid Valve Drive. *Mechanical and Electrical Information*, 2022(20): 48–51.
- [2] Wang Y, Tao G, Yang Y, 2014, Voltage and Temperature Compensation Control Method of Proportional Solenoid Valve. *Chinese Hydraulics & Pneumatics*, 2014(5): 86–89.
- [3] Angadi SV, Jackson RL, Choe S-Y, et al., 2009, Reliability and Life Study of Hydraulic Solenoid Valve. Part 2: Experimental Study. *Engineering Failure Analysis*, 16(3): 944–963. <https://doi.org/10.1016/j.engfailanal.2008.08.012>
- [4] Li J, Xiao M, Sun Y, et al., 2020, Failure Mechanism Study of Direct Action Solenoid Valve Based on Thermal-Structure Finite Element Model. *IEEE Access*, 8: 58357–58368. <https://doi.org/10.1109/ACCESS.2020.2982941>
- [5] Liu Y, Mao M, Xu X, et al., 2014, Thermodynamic Analysis of Multi Physical Field Coupling in Hydraulic Solenoid Valves. *Journal of Mechanical Engineering*, 50(2): 139–145.
- [6] Sun B, Liu L, Huang L, et al., 2019, Numerical Simulation and Experimental Research on the Thermal Physical Field of Electromagnetic Valves. *Hydraulic and Pneumatic*, 2019(5): 92–97.
- [7] Ren Y, Xi J, Chen H, et al., 2022, Analysis of Thermal Effects on Proportional Electromagnetic Valves for Vehicles Based on Hybrid Modeling Method. *Journal of Beijing Institute of Technology*, 42(3): 251–260.

### Publisher's note

Bio-Byword Scientific Publishing remains neutral with regard to jurisdictional claims in published maps and institutional affiliations.